Optical and magneto–optical properties of periodic Co double layer film*

Xia Wen-Bin(夏文斌)[a], Gao Jin-Long(高锦龙)[a], Zhang Shao-Yin(张绍银)[b], Chen Le-Yi(陈乐易)[a], Tang Yan-Mei(唐妍梅)[a], Tang Shao-Long(唐少龙)[a]†, and Du You-Wei(都有为)[a]

[a] *Nanjing National Laboratory of Microstructures, Department of Physics and Jiangsu Provincial Laboratory for Nanotechnology, Nanjing University, Nanjing* 210093, *China*

[b] *School of Science, Institute of Condensed Matter Physics, Linyi University, Linyi* 276005, *China*

(Received 22 April 2014; revised manuscript received 13 May 2014; published online 20 August 2014)

Co double layer film (CoDLF) consisting of a disk-array layer and an antidot-array layer, both with square order, was investigated. Both the reflectivity and Kerr spectra of CoDLF show anisotropic effects when the azimuthal angle of incident light changes. From the simulation result of surface plasmon polaritons (SPPs), we attribute the reflectivity minima and Kerr angle maxima in the spectra mainly to the excitation of different diffractional orders' SPPs. More interestingly, the Kerr angle changes sign at specific wavelengths. We attribute these phenomena to the excitation of SPPs and localized surface plasmons (LSPs), and the interaction between them.

Keywords: magneto-optics, surface plasmons, magneto-plasmonics

PACS: 33.57.+c, 73.20.Mf, 78.20.Ls, 85.70.Sq **DOI:** 10.1088/1674-1056/23/10/103303

1. Introduction

In the past few decades, the booming development of nanotechnology and the profound research findings in plasmonics, have reformed the traditional research field of magneto-optics into magneto-plasmonics, which focuses on the relationship between surface plasmons and magneto-optics.[1,2] In traditional studies of magneto–optical (MO) effects, people usually chose uniform film, either single layer or multi-layer, of ferromagnetic metals or dielectrics.[3] In recent years however, patterned structures with MO response have also captured the interest of researchers. Usually, patterned structures with periodic order can provide wavevector compensation between light in free space and SPPs, leading to the excitation of SPPs at the interface between a metal and a dielectric. The excitation of SPPs often results in the enhancement of an MO signal.[4–6] On the other hand, LSPs can also accumulate and redistribute electronic field near the metal surface. And unlike SPPs, LSPs can alter the sign of the Kerr angle, rather than only its magnitude.[7–10]

In a patterned system, people usually study its properties at symmetric positions, but often neglect the situation at arbitrary positions.[11] However, if we study the properties at arbitrary positions, some novel phenomena might be unveiled.[12] Moreover, the intermediate evolution between two symmetric positions is also interesting.

2. Sample fabrication

Our sample is fabricated mainly by interference lithography (IL) and magnetron sputtering. Although many methods are adopted in the research area of magneto-plasmonics, IL is a top–down method with unique advantages. Compared to other fabrication methods used to prepare periodic nanostructures, such as focused ion etching, electron beam lithography, and nanosphere lithography, IL has its own advantages, an excellent balance among low cost, long-range order, good reproducibility, and rapid production.

In this work, a 102-nm-thick positive photoresist (PR) (Allresist, AR P-3170) was spin-coated on a clean 1 cm×1 cm silicon wafer. After that the film was baked at 90 °C for 1 min. Then we adopted a Lloyd's Mirror system with a 442-nm wavelength He–Cd laser to implement interference lithography process. The PR film was exposed for 15 s. Then after rotating the sample around its normal axis, the PR film was exposed once again to form a square pattern. After developing in the developer (Allresist, AR 26-300), the orderly, square-symmetry disk-array pattern on PR film was obtained. The orderly pattern almost covered the entire wafer. The period of the ordered pattern is 400 nm on both the x and y axes, and the disk diameter is 285 nm. We removed the PR residue on the wafer surface by reactive ion etching. After magnetron-sputtering Co on the PR pattern, we got the Co double layer film (CoDLF). The thickness of the Co is 30 nm, which is thin enough to consider the Co film as double layer film instead of

*Project supported by the National Key Project of Fundamental Research of China (Grant Nos. 2012CB932304 and 2010CB923404), the National Natural Science Foundation of China (Grant Nos. 11374146 and U1232210), and the Priority Academic Program Development of Jiangsu Higher Education Institutions.

†Corresponding author. E-mail: tangsl@nju.edu.cn

© 2014 Chinese Physical Society and IOP Publishing Ltd

corrugated film.[13,14] As shown in Fig. 1(a), CoDLF has good periodicity which was reproduced from the PR pattern.

Figure 1(c) shows a schematic model of CoDLF, which clearly combines two layers. The bottom layer is an antidots film, which is a typical periodic metal film that is suitable for SPP excitation and propagation. On the other hand, in the top layer, although it has the same period, the disks are separated from each other; thus, they can be connected only through a free-space EM field, which could be excited as LSPs on each Co disk. The gap between disks is about 115 nm, which is too large to transport SPPs effectively, so the propagation of SPPs in the upper layer is much weaker than that of LSPs.

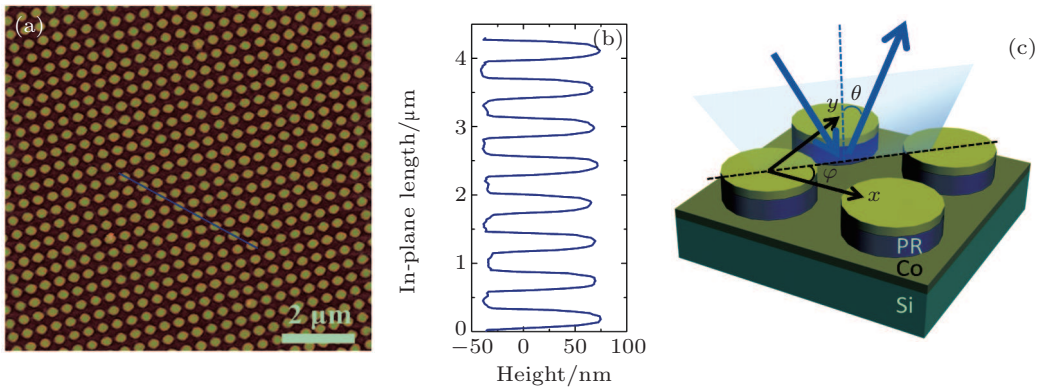


Fig. 1. (color online) (a) the CoDLF has good periodicity which was reproduced from the PR pattern. (b) Cross section outline of CoDLF. (c) The three-dimensional (3D) model of CoDLF. θ is the incident angle, φ is the azimuthal angle.

3. Simulation results

To excite SPPs, the SPP dispersion relations (1) and the wavevector matching conditions (2) for two-dimensional (2D) periodic lattices must be satisfied. The equations are written as

$$k_{\mathrm{spp}}(\lambda) = \frac{2\pi}{\lambda}\sqrt{\frac{\varepsilon_{\mathrm{d}}\cdot\varepsilon_{\mathrm{m}}}{\varepsilon_{\mathrm{d}}+\varepsilon_{\mathrm{m}}}}, \tag{1}$$

$$\left|\mathrm{Re}(k_{\mathrm{spp}}(\lambda))\right| = \left|\boldsymbol{k}_{\parallel}(\lambda) + m\cdot\frac{2\pi}{a}\boldsymbol{i} + n\cdot\frac{2\pi}{a}\boldsymbol{j}\right|, \tag{2}$$

where λ is the wavelength of incident light, ε_{d}, ε_{m} are the relative permittivities of the dielectric and the metal, $\mathrm{Re}(k_{\mathrm{spp}})$ is the real part of the wavevector of SPPs, a is period, $k_{\parallel}$ is the in-plane wavevector of incident light, and (m,n) are the two-dimensional diffractional orders of reciprocal lattice vectors.

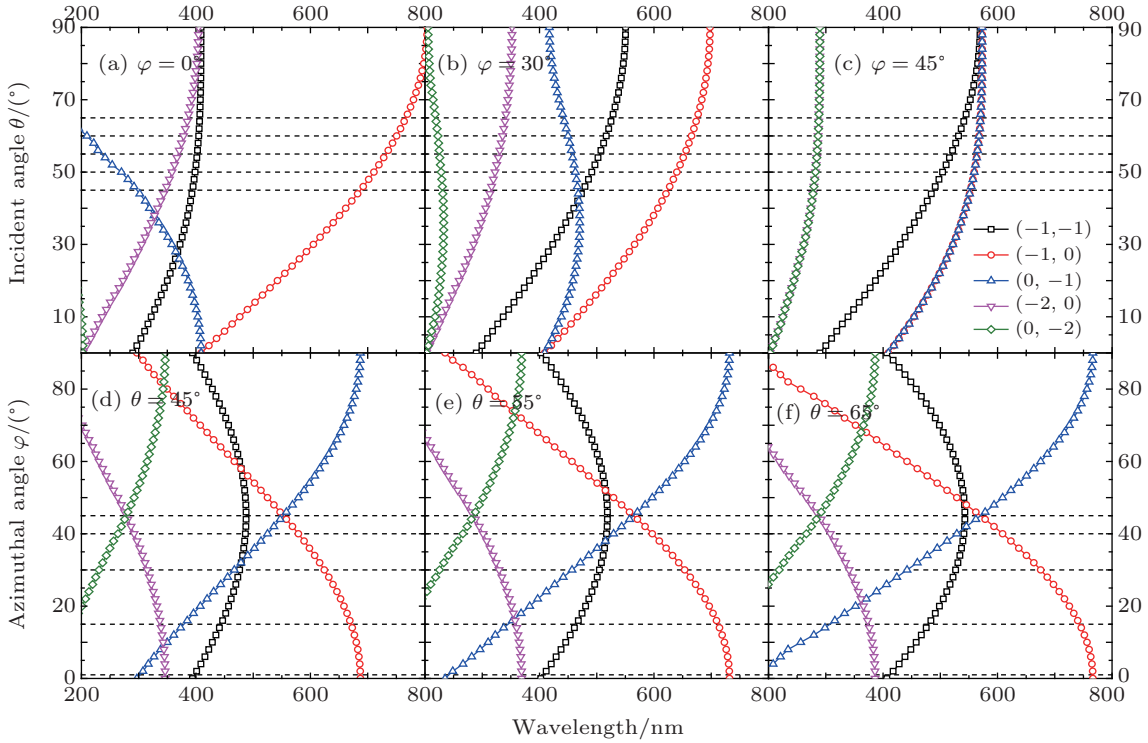


Fig. 2. (color online) Simulation results of incident light wavelengths that are needed to excite SPPs with different diffractional orders when (a) φ = 0°, (b) φ=30°, (c) φ = 45°, (d) θ = 45°, (e) θ=55°, (f) θ=65°. Dashed lines in panels (a)–(c) indicate the position at θ = 45°, 50°, 55°, 60°, 65°, while dash lines in panels (d)–(f) indicate the positions at φ = 0°, 15°, 30°, 40°, 45°.

Based on the equations, we calculate the specific wavelengths needed to excite SPPs with particular diffractional orders, namely (0, −1), (−1, 0), (−1, −1), (0, −2), (−2, 0).[15] The dielectric parameters of cobalt are taken from Ref. [16]. The calculated results are shown in Fig. 2. Because the pattern of CoDLF is two-dimensional, we introduce the azimuthal angle φ as the angle between incident plane and the in-plane x axis. Six situations are addressed: three azimuthal angles (0°, 30°, 45°) and three incident angles (45°, 55°, 65°), as shown in Fig. 1. In the visible range, we can see that only the three SPPs related to the (0, −1), (−1, 0), (−1, −1) diffractional orders (for simplicity, we call this kind of SPPs (m,n)-order SPPs) can be excited by light. Moreover, at $\varphi = 0°$ and $\theta = 45°$–$65°$, only (−1, 0), (−1, −1)-order SPPs can be excited, as shown in Fig. 2(a). At $\varphi = 45°$, the (−1, 0) and (0, −1), (−2, 0) and (0, −2)-order SPPs are degenerate because $\varphi = 45°$ is a symmetric position of a 2D square structure. This is also the reason for the symmetry of Figs. 2(d)–2(f) along the horizontal line $\varphi = 45°$.

On the other hand, the extinction, absorption, and scattering cross section of nanodisks were simulated by the discrete dipole approximation (DDA) method.[17] The shape and size of the nanodisk simulated are the same as for the nanodisk in the upper layer of our sample. The incident light is p-polarized and s-polarized respectively. The peak shown in both Figs. 3(a) and 3(b) around $\lambda = 850$ nm comes from LSPs oscillating along the disk surface. And the peak shown only in Fig. 3(a) around 300 nm is the LSPs oscillating between the two surfaces of the nanodisk. The peaks are mainly located out of the visible range; thus LSPs have relatively little effect on optical properties in this range.

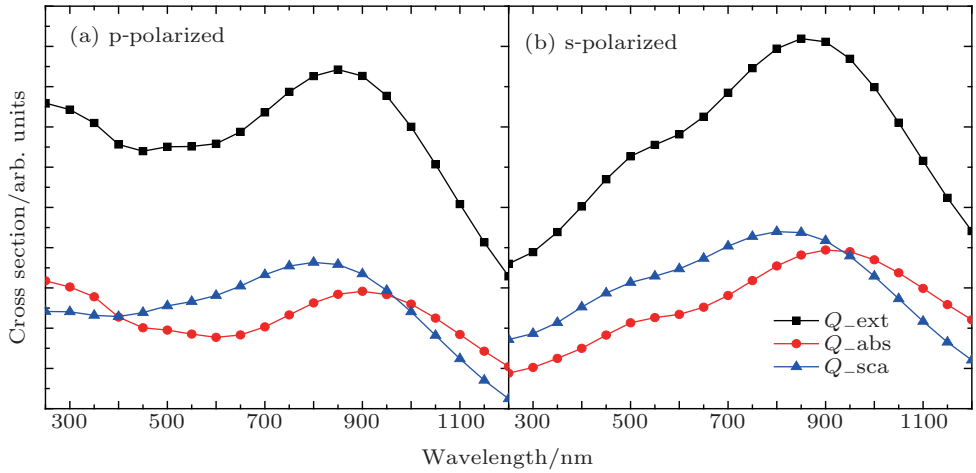


Fig. 3. (color online) DDA simulation results. The incident light is (a) p-polarized or (b) s-polarized. The incident angle is 45°. Q_ext, Q_abs, and Q_sca are the cross sections of extinction, absorption, and scattering respectively.

4. Experimental results

We measured the reflectivity of CoDLF at different incident angles and azimuthal angles for p-polarized light. Figure 4 shows the sample's reflectivity spectra with different incident angles but fixed azimuthal angle. Because the SPP nature of CoDLF dominates over the LSP nature, the reflectivity spectra are modified mainly by the excitation of SPPs.

As is well known, when the azimuthal angle changes, the matching condition for the excitation of SPPs also changes. At $\varphi = 0°$, as shown in Fig. 4(a), there is a dominant reflectivity minimum, which is also known as Wood's anomaly,[18] in the long-wavelength side of the spectrum. Referring to Fig. 2(a), we attribute this Wood's anomaly to the excitation of (−1, 0)-order SPPs distinctly. At the short wavelength side of the spectrum, the situation is much more complicated, because more than one order of SPPs is involved. At $\varphi = 0°$, three different orders of SPPs, (0, −1), (−1, −1), (−2, 0), work together to form the Wood's anomaly around $\lambda = 400$ nm. But in the range of 45°–65° of incident angles, (−1, −1)-order SPPs (black line in Fig. 2(a)) overwhelm other two orders.

At $\varphi = 30°$, as shown in Fig. 4(b), there are three Wood's anomalies. The strongest one is still from (−1, 0)-order SPPs, and the relatively weak ones are from (−1, −1)- and (0, −1)-order SPPs, respectively [see Fig. 2(b)]. At $\varphi = 45°$, the degenerated (−1, 0)- and (0, −1)-order SPPs dominate over the (−1, −1)-order SPPs; thus we see only one reflectivity minimum in Fig. 4(c).

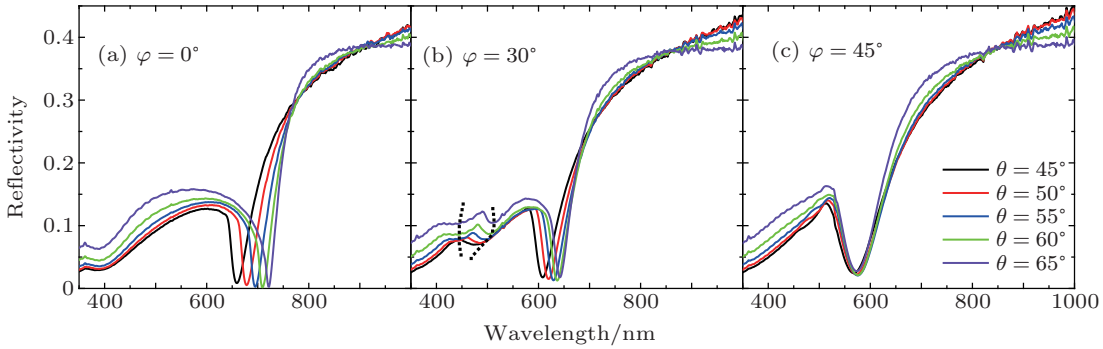


Fig. 4. (color online) Reflectivity spectra of CoDLF at $\theta = 45°$, $50°$, $55°$,$60°$, $65°$, at different azimuthal angles (a) $\varphi = 0°$, (b) $\varphi = 30°$, (c) $\varphi = 45°$. The incident light is p-polarized. The dotted lines in panel (b) indicate the position of two relatively weak reflectivity minima.

The longitudinal magneto–optical Kerr effect (MOKE) response of the system was measured with a custom-made MOKE measurement system, as shown in Fig. 5. We adopt the traditional idea of using beamsplitter to split light into signal light and reference light in order to measure the light intensities. We place the beamsplitter on the path of reflective light, instead of incident light, to avoid the reflectance fluctuation of the sample under different levels of magnetic field and obtain more accurate results.

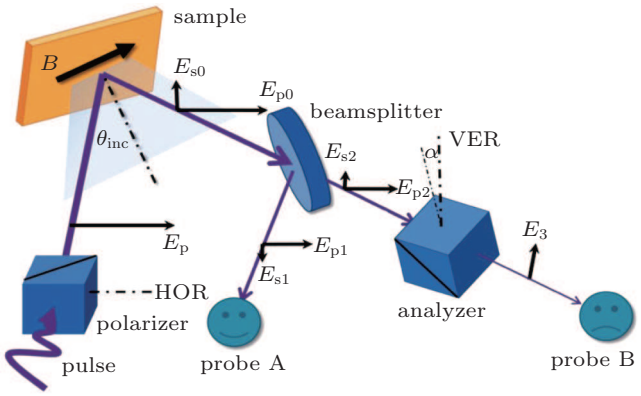


Fig. 5. (color online) Longitudinal MOKE measurement system. α is a small angle, which is the supplementary angle of the angle between polarization axes of analyzer and polarizer. Probe A receives the reference light, while probe B receives signal light.

The longitudinal Kerr angle spectra are shown in Fig. 6. The incident angle is fixed at 45° and the azimuthal angles are 0°, 20°, 30°, 40°, and 45°, respectively. The wavelength of incident light is among 430 nm–710 nm with the p-light configuration. As is well known, at the resonances of LSPs or SPPs, the signal of MOKE can be modified by the redistribution of the electromagnetic field at the vicinity of the metal–dielectric surface, which enhances the Kerr rotation, as is readily apparent in Fig. 6.

From Fig. 6(a), at $\varphi = 0°$, we can see that the Kerr angle changes its sign at $\lambda = 470$ nm. At $\varphi = 20°$, two Kerr angle peaks of opposite sign appear at the ends of the wavelength range, as shown in Fig. 6(b). At $\varphi = 40°$, there are three peaks in the MOKE spectrum, two at the positive side and one at the negative side. Similarly, in the Au disks/SiO_2/(Au/Co/Au) nano-structure, Torrado *et al.* observed similar transverse MOKE signals, and they called the peaks S-like and Peak-like shapes. They attributed the shapes to the SPPs from the Au/Co/Au trilayer and LSPs from Au disks, individually.[19] However, in our CoDLF, because the MOKE peaks shift as the azimuthal angle changes, the peaks cannot be attributed solely to LSPs. Consistent with Fig. 2(d) and Fig. 4, we propose that the positive peak at $\lambda = 480$ nm and $\varphi = 45°$ originates from the (0, −1)- and (−1, −1)-order SPPs, while the peak at $\lambda = 585$ nm comes from the (−1, 0)-order's SPPs.

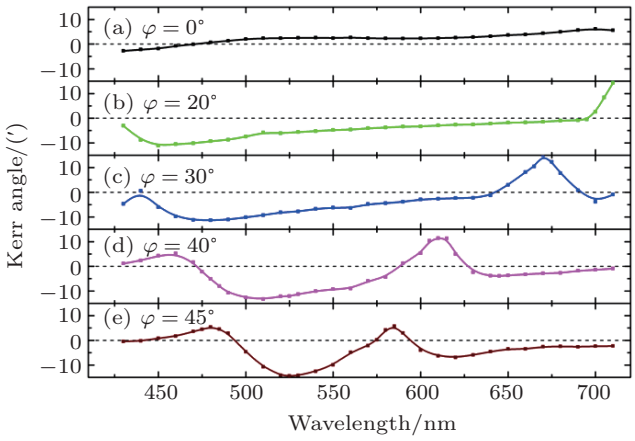


Fig. 6. (color online) Kerr angle spectra of longitudinal MOKE. The incident light is p-polarized. The saturation field is about 670 Oe (1 Oe = 79.5775 A·m^{-1}). The incident angle is 45°. The azimuthal angles are (a) 0°, (b) 20°, (c) 30°, (d) 40°, (e) 45° respectively.

In our previous work on Co antidot film (CoADF), though its period (400 nm) is slightly different from CoDLF, the Kerr spectra are similar.[15] Both of them have two peaks emerging at the two ends of spectra and moving towards each other with the azimuthal angle increasing. The Kerr angles of CoADF were simply enhanced at SPPs' excitation positions and kept

at the positive side for all azimuthal angles. However, the Kerr angles of CoDLF change their sign several times at certain azimuthal angles. For example, at $\varphi = 40^\circ$, the Kerr spectrum crosses zero at $\lambda = 472$ nm, 589 nm, and 627 nm (Fig. 6(d)). In the structural view, the difference between CoADF and CoDLF, and in turn the difference of their Kerr spectra, originates from the existence of the disk array at the top layer of CoDLF. Recently, Bonanni *et al.,* investigated how the polarizability of Ni disks affects the sign of Kerr angle through the excitation of LSPs, and they found that the Kerr angle changes its sign when the wavelength crosses over the position of the LSPs' resonance.[8] As for our sample, the position of the LSPs' resonance of the Co disks is around 850 nm (Fig. 3), which is out of the range of the Kerr spectra measured (430 nm–710 nm). Therefore the sign of the Kerr angle of CoDLF is not changed solely by LSPs, but it can be changed by the interactions between SPPs and LSPs. So the negative peak at $\lambda = 490$ nm in Fig. 6(c) is the result of the interaction between SPPs in the bottom layer and LSPs in the top layer. Though the positive peaks do not merge into a single peak as in CoADF, the maxima Kerr angle of CoDLF still reaches $15'$ both at the negative side ($\varphi = 45^\circ$, $\lambda = 525$ nm) and the positive side ($\varphi = 30^\circ$, $\lambda = 670$ nm), which is about 5 times that of pure Co film.

5. Conclusions

In conclusion, we have fabricated large-area Co double layer film with long-range order. The reflectivity spectra and the Kerr angle spectra show anisotropic effects with the azimuthal angle changing. The minima in the reflectivity spectra are related to the excitation of SPPs with different diffractional orders. The Kerr angle spectra are significantly modified by the interaction of SPPs and LSPs, and the maximum Kerr angle is reached in about $15'$.

References

[1] Barnes W L, Dereux A and Ebbesen T W 2003 *Nature* **424** 824

[2] Armelles G, Cebollada A, García-Martín A and González M U 2013 *Adv. Opt. Mater.* **1** 10

[3] Zhang S Y, Tang S L, Gao J L, Luo X J, Xia W B and Du Y W 2013 *Chin. Phys. B* **22** 087802

[4] Belotelov V I, Bykov D A, Doskolovich L L, Kalish A N, Kotov V A and Zvezdin A K 2009 *Opt. Lett.* **34** 398

[5] Chetvertukhin A V, Grunin A A, Baryshev A V, Dolgova T V, Uchida H, Inoue M and Fedyanin A A 2012 *J. Magn. Magn. Mater.* **324** 3516

[6] Belotelov V I, Akimov I A, Pohl M, Kotov V A, Kasture S, Vengurlekar A S, Gopal A V, Yakovlev D R, Zvezdin A K and Bayer M 2011 *Nat. Nanotechnol.* **6** 370

[7] Du G X, Mori T, Suzuki M, Saito S, Fukuda H and Takahashi M 2010 *Appl. Phys. Lett.* **96** 081915

[8] Bonanni V, Bonetti S, Pakizeh T, Pirzadeh Z, Chen J, Nogues J, Vavassori P, Hillenbrand R, Akerman J and Dmitriev A 2011 *Nano Lett.* **11** 5333

[9] Mayergoyz I D, Lang G, Hung L, Tkachuk S, Krafft C and Rabin O 2010 *J. Appl. Phys.* **107** 09A925

[10] Rubio-Roy M, Vlasin O, Pascu O, Caicedo J M, Schmidt M, Goni A R, Tognalli N G, Fainstein A, Roig A and Herranz G 2012 *Langmuir.* **28** 9010

[11] Papaioannou E T, Kapaklis V, Patoka P, Giersig M, Fumagalli P, Garcia-Martin A, Ferreiro-Vila E and Ctistis G 2010 *Phys. Rev. B* **81** 054424

[12] Torrado J F, Papaioannou E T, Ctistis G, Patoka P, Giersig M, Armelles G and Garcia-Martin A 2010 *Phys. Status Solidi-R* **4** 271

[13] Sapozhnikov M V, Gusev S A, Rogov V V, Ermolaeva O L, Troitskii B B, Khokhlova L V and Smirnov D A 2010 *Appl. Phys. Lett.* **96** 122507

[14] Sapozhnikov M V, Gusev S A, Troitskii B B and Khokhlova L V 2011 *Opt. Lett.* **36** 4197

[15] Xia W B, Gao J L, Zhang S Y, Luo X J, Chen L Y, Xu L Q, Tang S L and Du Y W 2014 *Opt. Express* **22** 1359

[16] Johnson P and Christy R 1974 *Phys. Rev. B* **9** 5056

[17] Draine B T and Flatau P J 1994 *J. Opt. Soc. Am. A* **11** 1491

[18] Wood R W 1902 *Phil. Mag.* **4** 396

[19] Torrado J F, Gonzalez-Diaz J B, Gonzalez M U, Garcia-Martin A and Armelles G 2010 *Opt. Express* **18** 15635